A Model for the Sensitivity of Non-Causal Control of Wave Energy Converters to Wave Excitation Force Prediction Errors

Francesco Fusco
Center for Ocean Energy Research (COER)
National University of Ireland Maynooth (NUIM)
Maynooth, Co. Kildare, Ireland
E-mail: francesco.fusco@eeng.nuim.ie

John V. Ringwood
Center for Ocean Energy Research (COER)
National University of Ireland Maynooth (NUIM)
Maynooth, Co. Kildare, Ireland
E-mail: john.ringwood@eeng.nuim.ie

***Abstract*—Wave Energy Converters (WECs) consisting of oscillating bodies can gain significant benefit from a real-time controller that is able to appropriately tune the system operation to the incident wave, thus allowing for a higher energy capture in a wider variety of wave conditions. Some of the proposed controllers, however, are non-causal and need predictions of the excitation force to be implemented in practise. A frequency-domain model is proposed, for the estimation of the effects that the wave- excitation-force prediction error has on the reference velocity that is calculated from the non-causal control law and, ultimately, on the absorbed power. The model can easily be derived exclusively from the predictor and from the non-causal law, with no additional information about the excitation force. Such a frequency-domain model can be valuable for the design of a robust control architecture, where the prediction error has a limited effect on the performance (power absorption). Focus is put on reactive control, but it is shown how the proposed sensitivity model can be generalised to other non-causal strategies, such as model predictive control.**

***Index Terms*—wave energy converter, control, wave forecasting.**

I. Introduction

Wave Energy Converters (WECs) consisting of oscillating bodies can gain significant benefit from a real-time controller that is able to appropriately tune the system operation to the incident wave, thus allowing for a higher energy capture in a wider variety of wave conditions. The ideal unconstrained control solution, that is reactive control [1], gives the conditions for the oscillating velocity and power take-off (PTO) force of the system such that maximum wave energy absorption is achieved, in any possible wave condition. Much attention, however, has been drawn by alternative control solutions where physical constraints are also accounted for in the optimisation process. Such solutions are usually based on model predictive control (MPC) [2], [3], [4], where the energy absorption over a finite receding time-horizon is maximised, taking into account limitations on the system's motion and PTO machinery forces.

Both reactive control and MPC, however, require prediction of the wave excitation force to be implemented in practise. Short-term wave forecasting was studied either with a deterministic approach [5]–[7], and as a purely stochastic univariate time series problem [8], [9]. In the latter, in particular, it is demonstrated how accurate predictions of the low-frequency wave components, for more than one mean wave period ahead, can be achieved with simple linear autoregressive (AR) models. Such models are also valid for the prediction of the wave excitation force, which is the effect of the incident wave elevation on the floating system, that results from the application of a low-pass filter. Whatever the selected prediction model is, however, an error is inevitably introduced, and this can negatively affect the performance of the controller.

This study presents a methodology for the quantification of the sensitivity of reactive control and MPC to the excitation force prediction error. A general structure of the real-time controller is firstly introduced, in section II, where a non-causal law, based on MPC or reactive control, is utilised for the calculation of the optimal velocity that the WEC should have for maximum power absorption. Tracking of this velocity reference, which in practise would be achieved by some lower-level control loop, is assumed perfect here.

A frequency-domain model of the propagation of the prediction error into the reference velocity and, ultimately, into the loss of power absorption, is then proposed in section III. Although only valid for linear control strategies, like reactive control and unconstrained MPC, such a frequency-domain interpretation of the sensitivity to the wave-excitation-force prediction error can be extremely valuable. Guidelines for the design of the prediction model and of the velocity tracking control loop can, in fact, be derived such that the influence of the prediction error on the performance (power absorption) is reduced.

In section IV, the introduced methodology is proven, by simulating an ideal WEC, consisting of a floating cylinder constrained to move in one degree of freedom. The main conclusions are finally outlined in section V.

II. Real-time Control of a heaving buoy

The wave-energy conversion system considered in this study consists of a generic floating body, oscillating in heave. The

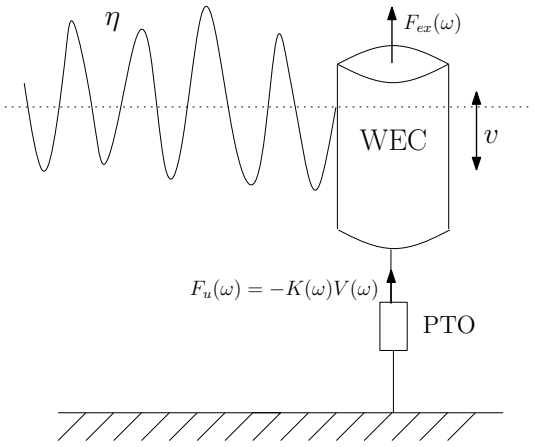

Fig. 1. A floating cylinder oscillating in heave.

relative motion with respect to the sea bottom is converted into useful electricity by a power take-off (PTO) mechanism, which is left unspecified at this stage. The motion of such a system, schematised in Fig. 1, is described by the following dynamic equation:

$$M\dot{v}(t) + \int_0^t z(t-\tau)v(\tau)d\tau + K_f v(t) + K_s x(t) = f_{ex}(t) + f_u(t), \quad (1)$$

where M is the mass of the body, $v(t)$ and $x(t)$ its velocity and position, $z(t)$ is the kernel function modelling the radiation impedance, K_f is a constant loss resistance and K_s is the restoring coefficient (modelling the linear restoring force resulting from the balance between buoyancy and weight). The external forces acting on the systems are the excitation force, $f_{ex}(t)$, due to the incident waves, and a controllable load force, $f_u(t)$, produced by the PTO. Note that Eq. (1) is valid under the assumption of zero initial conditions, that is $x(0) = v(0) = 0$.

The model of the WEC, as linearity is assumed for all the hydrodynamic forces, can alternatively be expressed in the frequency domain:

$$Z_i(\omega)V(\omega) = F_{ex}(\omega) + F_u(\omega), \quad (2)$$

where all the properties of the system are conveniently incorporated in the intrinsic mechanical impedance, $Z_i(\omega)$, defined as:

$$Z_i(\omega) = B(\omega) + K_f + \jmath\omega\left[M + M_a(\omega) - \frac{K_s}{\omega^2}\right]. \quad (3)$$

In Eq. (3), the Fourier transform of the radiation kernel is expressed as $\mathscr{F}\{z(t)\} = B(\omega) + \jmath\omega M_a(\omega)$, in terms of the radiation resistance, $B(\omega)$, and the added mass, $M_a(\omega)$. Note that such a Fourier transform is only valid in a generalised sense, as $M_a(\omega)$ does not, in general, vanish in the limit $\omega \to +\infty$ [1].

The excitation force, $f_{ex}(t)$, is the effect that the incident wave elevation, $\eta(t)$, has on the system, determined by the non-causal excitation transfer function $H_{ex}(\omega)$ [1]:

$$F_{ex}(\omega) = H_{ex}(\omega)\Xi(\omega) \quad (4)$$

Note that in Eq. (4), $\Xi(\omega)$ represents the Fourier transform of the wave elevation, $\Xi(\omega) = \mathscr{F}\{\eta(t)\}$.

The average power absorbed by the system, over the time T, is:

$$P_u = -\frac{1}{T}\int_0^T f_u(t)v(t)dt, \quad (5)$$

which can be equivalently expressed in the frequency domain by using Parseval's theorem [1]:

$$P_u = -\frac{1}{2\pi T}\int_0^\infty F_u(\omega)V^*(\omega) + F_u^*(\omega)V(\omega)d\omega. \quad (6)$$

The notation $(\cdot)^*$ indicates the complex-conjugate operation. Note that the Parseval's theorem can only be applied if the force and velocity signals, $f_u(t)$ and $v(t)$, are supposed to be zero outside the time interval $[0,\, T]$.

The control objective is to opportunely tune the system's motion so that the wave power absorption is maximised, eventually accounting for any constraint that may be imposed by physical realisability (e.g. motion/force constraints) or by other practical considerations. A general control framework is represented in the blocks scheme of Fig. 2. From measurements (or estimates) of the excitation force, a reference oscillation velocity is calculated according to a certain higher-level control (HLC) logic. A lower-level control (LLC) loop then imposes the desired velocity on the WEC, by acting on the PTO force. The reference generation can be based on analytical solutions, like for example reactive control [1], or numerical optimisation algorithms which may additionally include constraints, MPC being the best example of such a category [2], [3], [4]. As also highlighted in the control scheme of Fig. 2, the reference generator requires, in general, predictions of the excitation force. Such requirements depend on the actual control strategy and on the specific system to be controlled [10], but it is widely recognised that they are usually necessary [10], [11], [12], [13], [2]. Note, however, that there is also the possibility to implement suboptimal but causal control strategies, where only current and/or past values of the excitation force are utilised to determine the reference velocity [14], [15].

It is important to mention, here, that other architectures have been proposed where the velocity is not controlled directly, but the PTO force is optimised and imposed on the system in a feed-forward fashion [16], [14]. Such solutions, in the authors opinion, may loose their effectiveness in a real-world implementation, where inaccuracies in the model (non-linearities, uncertainties in the parameters or prediction errors) could lead to poor control actions. Unless a very accurate (non-linear) model is utilised in the optimisation, the velocity resulting from application of such a force may not be the one expected, thus leading to a performance drop. Inclusion of the velocity in the control loop, on the other hand, allows a more robust correction of the effects of unknown (or non-modelled)

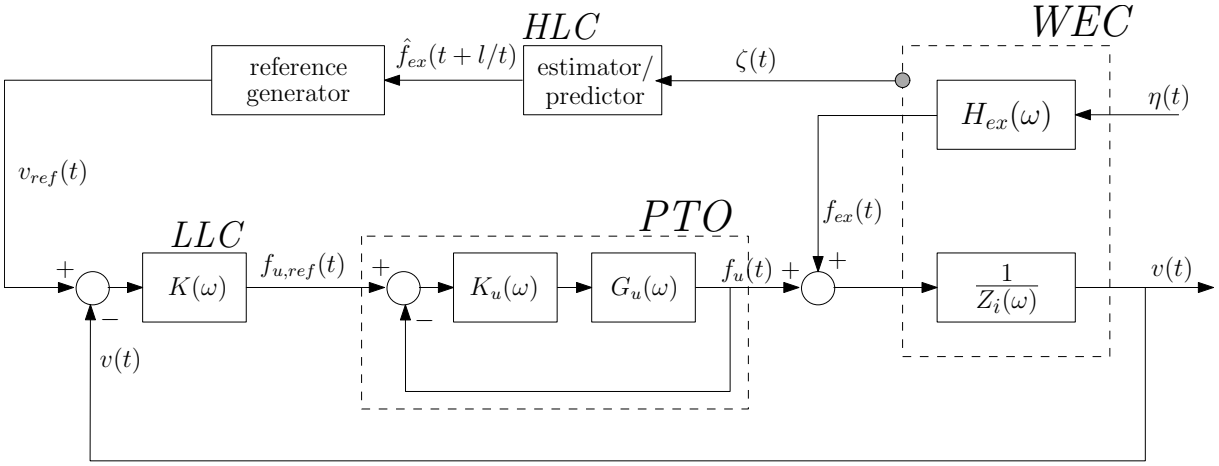

Fig. 2. General structure for a real-time controller of a WEC.

components of the system. Note that the control objective is usually to amplify the motion of the system (for maximum wave energy absorption), which goes against the assumption of small motions that is behind the linear models commonly utilised for the control system design.

In the remainder of this section, two non-causal reference-generation strategies are outlined: reactive control and MPC. These well known case studies will serve for the introduction of a methodology that can be used in order to determine the effects that excitation-force prediction errors can have on the reference velocity and ultimately on the performance of the control system, that is the power capture.

A. Unconstrained Reactive Control

It was demonstrated [1] that maximum average power is transferred from the waves to the system under the two following conditions:

$$V_{opt}(\omega) = \frac{1}{2B(\omega) + 2K_f} F_{ex}(\omega) \tag{7}$$

$$F_{u,opt}(\omega) = -Z_i^*(\omega)V(\omega) = -\frac{Z_i^*(\omega)}{2B(\omega) + 2K_f} F_{ex}(\omega), \tag{8}$$

which we term optimal velocity, $V_{opt}(\omega) = \mathscr{F}\{v_{opt}(t)\}$, and optimal load force, $F_{u,opt}(\omega) = \mathscr{F}\{f_{u,opt}(t)\}$.

Within the control framework that is assumed in this paper, as shown in Fig. 2 and described in section II, the condition of Eq. (7) is implemented by the reference generator to calculate the reference velocity from estimates/measurements of the excitation force. At time t:

$$v_{opt}(t) = \int_{-\infty}^{+\infty} h_{opt}(\tau) f_{ex}(t-\tau) d\tau, \tag{9}$$

where

$$h_{opt}(t) = \mathscr{F}^{-1}\left\{\frac{1}{2B(\omega) + 2K_f}\right\} = \mathscr{F}^{-1}\left\{H_{opt}(\omega)\right\}. \tag{10}$$

Note that the Fourier inversion of Eq. (10) is only valid in a generalised sense, as explained in [10]. The function $H_{opt}(\omega)$, in fact, tends to the constant $1/2K_f$ at low and high frequencies, so that the kernel function $h_{opt}(t)$ can be decomposed as:

$$h_{opt}(t) = \frac{1}{2K_f}\delta(t) + k(t), \tag{11}$$

where $\delta(t)$ is a Dirac delta function and

$$k_{opt}(t) = \mathscr{F}^{-1}\left\{H_{opt}(\omega) - \frac{1}{2K_f}\right\} = \mathscr{F}^{-1}\left\{K_{opt}(\omega)\right\}. \tag{12}$$

After the singularity of the kernel function $h_{opt}(t)$ is isolated, the Fourier transform in Eq. (12) is now well defined, as $K_{opt}(\omega)$ tends to zero for high and low frequencies.

By combining Equations (9) and (11), the optimal reference velocity is finally given by:

$$v_{opt}(t) = \frac{1}{2K_f} f_{ex}(t) + \int_{-\infty}^{t} k_{opt}(\tau) f_{ex}(t-\tau) d\tau. \tag{13}$$

It is well known, however, that the kernel function $h_{opt}(t)$, and therefore $k_{opt}(t)$, is non-causal [11], [1]. In particular, $h_{opt}(t)$ and $k_{opt}(t)$ are real and even functions. This means that evaluation of the convolution of Eq. (13) requires past as well as future values of the excitation force. Moreover, values infinitely far into the future need to be known, as the convolution starts from $\tau = -\infty$. The kernel function $k_{opt}(t)$, however, tends to zero and can be neglected after some time, so that only a finite future (and past) time horizon is required, in practise, for the calculation of the optimal velocity. In [17] and [10], in particular, a methodology is introduced to determine the finite prediction horizon over which the excitation force must be known in order to approach the optimal velocity within a certain degree of accuracy.

Considering also that the actual implementation of the reference generator has to be in discrete time, the optimal reference velocity, based on reactive control, is ultimately calculated as:

$$v_{opt}[k] \approx \frac{1}{2K_f} f_{ex}[k] + T_s \sum_{j=-L}^{L} k_{opt}[j] f_{ex}[k-j], \tag{14}$$

where T_s is the sampling time and L is the future (and past) horizon after which additional knowledge of the excitation force has no significant influence on the velocity calculation.

B. Model Predictive Control

The optimal velocity given by reactive control is based on the minimisation of the average power at every frequency, over an infinite time horizon. MPC, on the other hand, optimises the operation of the system (velocity and/or force) such that the average power, or the energy, over a *finite* future horizon, is maximum. In particular, at each time step k, the following functional is maximised, over a given time horizon L,:

$$J[k] = -\sum_{j=1}^{L} f_u[k+j]v[k+j], \tag{15}$$

possibly subject to constraints on the system's variables. Note that the length of the receding horizon, L, has a different meaning that the quantity L used in Eq. (14), for the calculation of the optimal velocity with reactive control. In both cases, however, L indicates the prediction horizon required for a practical implementation, and that's why the same symbol has been adopted.

In the presence of constraints, an explicit solution for the transfer function between reference velocity and excitation force cannot be found, in general. The discussion, here, focuses on the unconstrained solution, which allows the expression of the reference velocity as a linear function of the excitation force (future and past), just as found for reactive control, in Eq. (14). Such a solution is immediately derived if a state space model for the floating system is available. For this purpose, a finite-order approximation of the radiation convolution of Eq. (1) is required, as this is only known numerically from some hydrodynamic software (refer to [18], [19] for details on radiation identification of floating structures).

Suppose that the following discrete-time model of the radiation force has been identified:

$$\begin{cases} z_r[k+1] = A_r z_r[k] + B_r v[k] \\ f_r[k] = C_r z_r[k] \end{cases}, \tag{16}$$

where $f_r[k]$ is the radiation force, $v[k]$ is the system's velocity and $x_r[k]$ is a state variable whose dimension represents the order of approximation. Note that the system in Eq. (16) does not exactly represents the radiation force but only its component after the singularity of the added mass at infinite frequency is removed [4]. Based on Eq. (16), the unconstrained minimum of the functional in Eq. (15) is found by adapting the results from [4]:

$$\tilde{v}_{opt}[k] = \frac{1}{2}\left(\Gamma + K_f I\right)^{-1}\left(-\tilde{F}_r \tilde{z}_r[k] + \tilde{f}_{ex}[k]\right). \tag{17}$$

where, all the signals have expressed as extended vectors over the future horizon L:

$$\begin{aligned} \tilde{v}_{opt}[k] &= \begin{pmatrix} v_{opt}[k+1] & \dots & v_{opt}[k+L] \end{pmatrix}^T \\ \tilde{z}_r[k] &= \begin{pmatrix} z_r[k+1]^T & \dots & z_r[k+L]^T \end{pmatrix}^T \\ \tilde{f}_{ex}[k] &= \begin{pmatrix} f_{ex}[k+1] & \dots & f_{ex}[k+L] \end{pmatrix}^T, \end{aligned} \tag{18}$$

and the matrices Γ and $\tilde{F}_r$ only depends on the radiation system:

$$\tilde{F}_r = \begin{pmatrix} C_r A_r \\ C_r A_r^2 \\ \dots \\ C_r A_r^L \end{pmatrix} \qquad \Gamma = \frac{1}{2}\left(\tilde{G}_r + \tilde{G}_r^T\right), \tag{19}$$

with

$$\tilde{G}_r = \begin{pmatrix} C_r B_r & 0 & \dots & 0 \\ C_r A_r B_r & C_r B_r & \dots & 0 \\ \vdots & & \ddots & \vdots \\ C_r A_r^{L-1} B_r & C_r A_r^{L-2} B_r & \dots & C_r B_r \end{pmatrix}. \tag{20}$$

Note that $(\cdot)^T$ denotes the transposed of a vector or matrix and I, in Eq. (17), is the identity matrix.

At each instant k we are only interested in forcing the system to follow the first value of the optimal vector $\tilde{v}_{opt}[k]$, that is $v_{opt}[k+1]$ (at the following instant, $k+2$, a new optimisation is performed). Therefore, the reference-generation strategy is actually:

$$\begin{aligned} v_{opt}[k+1] = H\tilde{f}_{ex}[k] - H\tilde{F}_r z_r[k] = \\ \sum_{j=1}^{L} h_j f_{ex}[k+j] + \sum_{j=1}^{L} h_j C_r A_r^j z_r[k], \end{aligned} \tag{21}$$

where

$$\begin{aligned} H = \begin{pmatrix} 1 & 0 & \dots & 0 \end{pmatrix} \frac{1}{2}\left(\Gamma + K_f I\right)^{-1} = \\ \begin{pmatrix} h_1 & h_2 & \dots & h_L \end{pmatrix} \end{aligned} \tag{22}$$

Note the similarity of the reference generation for reactive control, Eq. (14), with the solution of the unconstrained MPC, Eq. (21). In the latter, the past values of the excitation force are accounted for in the term depending on the radiation state variable, $z_r[k]$. The future horizon L is determined by the time horizon chosen for the optimisation. One may expect that MPC will converge towards reactive control if an infinitely (or sufficiently) long horizon L is considered.

III. Effects of prediction errors on control performance

Within the general control framework proposed in section II, and schematised in Fig. 2, the velocity reference is generated from predictions of the excitation force. This study aims at the definition of a methodology that would aid the quantification of the effects that the inevitable prediction errors have on the reference velocity and ultimately on the control performance (absorbed power). Having a proper understandings of these effects would make it possible to increase the robustness of the control, by acting on the reference-generation logic or on the lower-level control. From this perspective, a frequency-domain interpretation of the mapping between excitation-force prediction error and velocity reference is of particular interest. The latter is introduced in section III-B, after the excitation-force prediction error is characterised in section III-A. Section III-C, then, analyses how the error propagates

from the reference velocity to the power absorption of the system.

Note that, while the focus is maintained on the two reference-generation strategies outlined in section II, based on reactive control and MPC, the methodology presented here can be extended to other possible linear control approaches.

A. Characterisation of excitation-force prediction error

At every instant k, the future values of the excitation force are approximated through some prediction model:

$$\hat{f}_{ex}[k+l|k] = f_{ex}[k+l] + \hat{e}[k+l|k], \tag{23}$$

where $\hat{f}_{ex}[k+l|k]$ is the l-step ahead prediction and $\hat{e}[k+l|k]$ is the prediction error.

If a stochastic time series model is utilised as a predictor, the one-step ahead prediction is usually calculated as a combination, not necessarily linear (e.g. neural networks), of past values of the excitation force:

$$\hat{f}_{ex}[k+1|k] = \varphi\big(f_{ex}[k],\, f_{ex}[k-1],\, \dots\, f_{ex}[k-n]\big), \tag{24}$$

where $\varphi(\cdot)$ is an unspecified function. The multi-step predictions are then determined recursively as:

$$\begin{aligned}\hat{f}_{ex}[k+l|k] = \varphi\big(&\hat{f}_{ex}[k+l-1|k],\\ &f_{ex}[k+l-2], \dots\, f_{ex}[k-n+l-1]\big).\end{aligned} \tag{25}$$

The one-step ahead prediction error, $\hat{e}[k+1|k]$, can be assumed to be a white noise with zero mean and variance σ^2:

$$\hat{e}[k+1|k] \sim \aleph(0, \sigma^2). \tag{26}$$

The assumption in Eq. (26) is reasonable if the prediction model accurately captures all the dynamics of the real system. The multi-step ahead prediction errors, however, for the recursive nature of the predictor, will be a combination of white noises and, therefore, colored noise, which can be described by its spectral density. Particularly for a linear predictor, it is quite straightforward to derive the spectral model of the prediction error.

Suppose that an AR prediction model, which was shown to be suitable for wave forecasting [9], is utilised:

$$\hat{f}_{ex}[k+1|k] = \sum_{j=1}^{n} a_j f_{ex}[k+1-j] + \zeta[k+1], \tag{27}$$

where a_j, with $j = 1, \dots n$, are the parameters of the model and $\zeta[k]$ is white noise. The multi-step ahead prediction error resulting from an AR model is a moving average system [20]:

$$\begin{aligned}\hat{e}[k+l|k] &= \sigma F^l(z)\zeta[k+l] = \\ &\sigma\left(1 + f_1 z + \dots + f_{l-1} z^{l-1}\right)\zeta[k+l] = \\ &\sigma\left(\zeta[k+l] + f_1\zeta[k+l-1] + \dots + f_{l-1}\zeta[k+1]\right),\end{aligned} \tag{28}$$

where z is the discrete complex frequency and the coefficient of the transfer function $F^l(z)$ are directly calculated from the parameters of the AR model. In particular $F^l(z)$ derives from the following identity [20]:

$$1 = A(z)F^l(z) + z^l G(z), \tag{29}$$

where it can be calculated as the quotient when dividing 1 by $A(z)$. In Eq. (29), the coefficients of $A(z)$ are the parameters of the AR model, a_j, while the term $z^l G(z)$ is the remainder of the polynomial division.

The variance of the multi-step ahead prediction error is easily calculated as:

$$\begin{aligned}E\left\{\hat{e}[k+l|k]^2\right\} = \left(1 + f_1^2 + \dots + f_{l-1}^2\right)\sigma^2 = \\ \sigma^2 \int_0^{\pi} \frac{F^l(e^{-\jmath\omega})F^l(e^{\jmath\omega})}{\pi} d\omega.\end{aligned} \tag{30}$$

Note that the absolute value squared of the transfer function $F^l(z)$ represents the spectral distribution of the l-step ahead prediction error, that is how this error is distributed in the frequency domain.

B. Effects of prediction errors on the reference velocity

The two velocity-reference-generation strategies based on reactive control, in Eq. (14), and MPC, Eq. (21), can both be written in the following general form:

$$v_{ref}[k] = v_{ref}^{(c)}[k] + \sum_{j=-L}^{-1} h_{ref}[j] f_{ex}[k-j], \tag{31}$$

where $v_{ref}^{(c)}$ denotes the causal part of the calculation of the reference velocity and $h_{ref}[j]$ is the impulse response function of the reference generator, whose specific values depend on the strategy adopted. Note that for reactive control the causal part is the convolution involving current and past values of the excitation force, while in the case of MPC it involves current and past values of the radiation state variable (which ultimately depend on the excitation force).

What is of interest, here, is to understand how the prediction error maps into the reference velocity and possibly to give a frequency-domain interpretation of this transfer. The actual reference velocity calculated from predicted values is:

$$\begin{aligned}\hat{v}_{ref}[k] &= v_{ref}[k] + \Delta v_{ref}[k] = \\ &v_{ref}^{(c)}[k] + \sum_{j=-L}^{-1} h_{ref}[j]\hat{f}_{ex}[k-j|k] = \\ &v_{ref}[k] + \sum_{j=-L}^{-1} h_{ref}[j]\hat{e}[k-j|k],\end{aligned} \tag{32}$$

where $\Delta v_{ref}[k]$ denotes the deviation from the desired velocity, due to the prediction error, $\hat{e}[k+l|k]$, whose expression was given in Eq. (23).

By introducing the model of the prediction error, Eq. (28), the error in the reference is readily written as a stochastic process driven by a white noise representing the one-step ahead prediction error:

$$\Delta v_{ref}[k] = \sum_{j=-L}^{-1} h_{ref}[j]\sigma F^{-j}(z)\zeta[k-j] \tag{33}$$

It is straightforward to verify that the reference-velocity error model, in Eq. (33), is a moving average stochastic process:

$$\begin{aligned}\Delta v_{ref}[k] &= \sigma G^L(z)\zeta[k+L] = \\ &\sigma\left(g_0 + g_1 z + \cdots + g_{L-1}z^{L-1}\right)\zeta[k+L] = \\ &\sigma\left(g_0\zeta[k+L] + g_1\zeta[k+L-1] + \cdots + g_{L-1}\zeta[k+1]\right),\end{aligned} \tag{34}$$

where the coefficients of the filter $G(z)$ are calculated from the reference generation impulse response function, $h_{ref}[k]$, and from the multi-step ahead error model, $F^l(z)$, as:

$$\begin{aligned}g_0 &= h_{ref}[-L] \\ g_1 &= h_{ref}[-L]f_1 + h_{ref}[-L+1] \\ \cdots &\qquad \cdots \\ g_{L-1} &= h_{ref}[-L]f_{L-1} + \cdots + h_{ref}[-2]f_1 + h_{ref}[-1].\end{aligned} \tag{35}$$

The absolute squared value of the filter $G(z)$ represent the spectral distribution of the error in the velocity reference and the total variance is:

$$\begin{aligned}E\left\{\Delta v_{ref}[k+l|k]^2\right\} = \left(g_0^2 + g_1^2 + \cdots + g_{L-1}^2\right)\sigma^2 = \\ \sigma^2\int_0^\pi \frac{G^L(e^{-\jmath\omega})G^L(e^{\jmath\omega})}{\pi}d\omega.\end{aligned} \tag{36}$$

By using Equations (34) and (36) it is possible, given the prediction model and the characteristics of the one-step ahead prediction error, to estimate the error in the reference velocity and its frequency distribution.

C. Effect of errors in the reference velocity on the performance

The error in the reference velocity, produced by incorrect estimates of the future excitation force, causes a velocity, which is different from the desired one, to be imposed on the system. Tracking the incorrect reference, through the lower level control loop, can result in a performance drop, that is a loss of power absorption. In this section, the effect of the error in the reference velocity on the average power absorption is quantified with a frequency-domain interpretation.

Within the scope of this study, focus is put on reactive control, which allows for the derivation of a simple analytical model in the frequency domain. In particular, the power loss due to error in the velocity reference is calculated as deviation from the ideal unconstrained optimal power achievable with reactive control. In the case of MPC, even if unconstrained, such model is not as straightforward to derive and it is left for further studies.

The spectral density of the absorbed power, from Eq. (6), is:

$$P_u(\omega) = \frac{1}{2\pi T}\left[F_u(\omega)V^*(\omega) + F_u^*(\omega)V(\omega)\right], \tag{37}$$

and represents the average power absorbed at each frequency, in $W \cdot s/rad$. In the case of reactive control, the spectral density of the maximum average power absorbed, is:

$$P_{opt,u}(\omega) = -\frac{1}{\pi T}B(\omega)|V_{opt}(\omega)|^2, \tag{38}$$

where Equations (8) and (7) were utilised. As a result of the prediction error, the following velocity, in the frequency domain, is actually imposed on the system:

$$\hat{V}_{opt}(\omega) = V_{opt}(\omega) + \Delta V_{opt}(\omega), \tag{39}$$

as from Eq. (33). The actual absorbed power is therefore:

$$P_u(\omega) = \frac{1}{2\pi T}\left[\hat{F}_u(\omega)\hat{V}_{opt}^*(\omega) + \hat{F}_u^*(\omega)\hat{V}_{opt}(\omega)\right], \tag{40}$$

where $\hat{F}_u(\omega)$ is the load force that is applied by the PTO on the floating system to impose the (incorrect) velocity reference:

$$\hat{F}_u(\omega) = Z_i(\omega)\left[V_{opt}(\omega) + \Delta V(\omega)\right] - F_{ex}(\omega), \tag{41}$$

which is based on the model of the system, Eq. (2).

By substituting Equations (39) and (41) in Eq. (40), it is possible to show that:

$$P_u(\omega) = -\frac{1}{\pi T}B(\omega)|V_{opt}(\omega)|^2 + \frac{1}{\pi T}B(\omega)|\Delta V(\omega)|^2. \tag{42}$$

At each frequency, the average power loss is proportional to the absolute value squared of the error in the velocity reference. In particular, in relative terms:

$$\frac{P_{opt}(\omega) - P_u(\omega)}{P_{opt}(\omega)} = \frac{|\Delta V(\omega)|^2}{|V_{opt}(\omega)|^2}. \tag{43}$$

Note that, by using Eq. (34):

$$|\Delta V(\omega)|^2 = \sigma^2 G^L(e^{-\jmath\omega})G^L(e^{\jmath\omega}), \tag{44}$$

which represents the spectral distribution of the variance of the reference velocity error, as shown in Eq. (36).

A frequency-domain model for the power drop due to inaccuracies in the reference velocity, produced by excitation-force prediction errors, has therefore been found. In particular, the average power loss, at each frequency, is proportional, through the system's radiation, to the spectral density of the velocity error, which is easily determined, Eq. (39), from the spectral distribution of the one-step ahead prediction error, the parameters of the predictor and the reference-generation kernel function.

IV. Results and discussion

The validity of the frequency-domain models, introduced in section III, for the estimation of effects of excitation-force prediction error on the velocity reference and on the power absorption, is verified here. A wave-energy conversion system consisting of a floating cylinder, as described in section II, is considered. Its geometry is defined by the radius $R = 5\,m$, the height $H = 25\,m$ and the draught $h = 20\,m$. The radiation and excitation characteristics are shown in Fig. 3 and were identified with the aid of the hydrodynamic software Wamit [21].

Reactive control was implemented, as outlined in section II-A, for two different wave systems, which come from real data collected at the Belmullet wave-energy test site, off the West coast of Ireland. In particular, a wave field consisting of a well defined swell centered at low frequencies and a

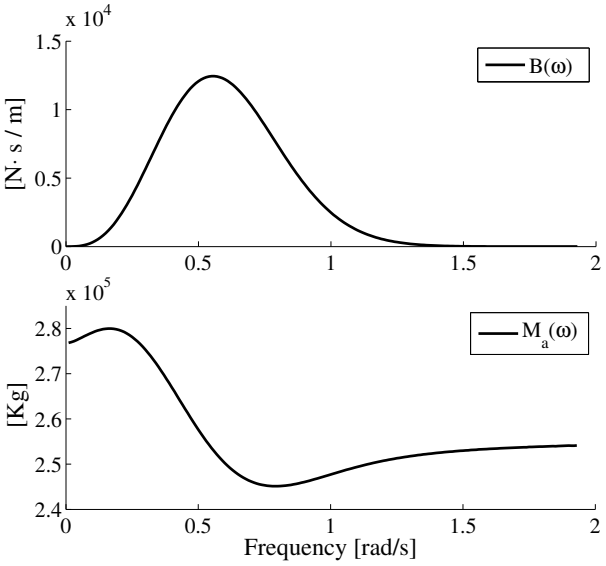

(a)

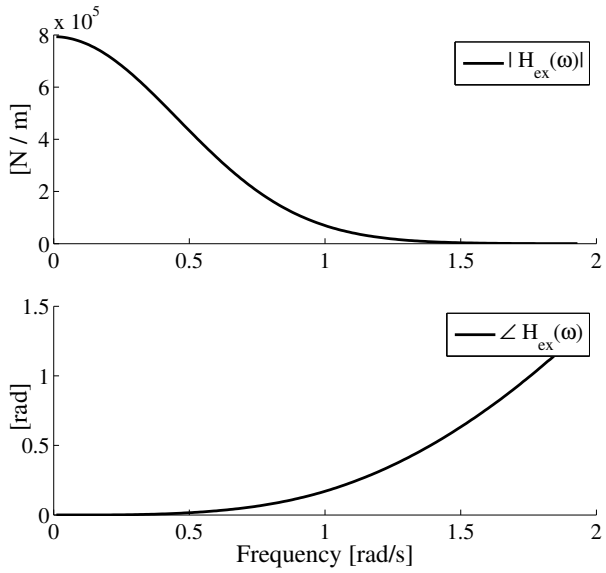

(b)

Fig. 3. Frequency response of the selected floating cylinder, with radius $R = 5\,m$, height $H = 25\,m$ and draught $h = 20\,m$.

wider-band sea state, centered at higher frequencies, were selected. The two data sets consist of 2304 measurements with a sampling rate of $1.28\,Hz$, but they were interpolated and the calculations were all performed (to increase the accuracy) at $2.56\,Hz$. The wave-energy spectrum of the selected sea states is shown in Fig. 4, along with the spectrum of the corresponding excitation force produced on the WEC.

According to the methodology presented in [10], a prediction horizon of $L = 150$ steps (almost $60\,s$ at $2.56\,Hz$) was chosen, for the implementation of the non-causal law in Eq. (14). In particular such a prediction horizon is required for a very close approximation of the optimal velocity that the system should follow for maximum wave energy absorption.

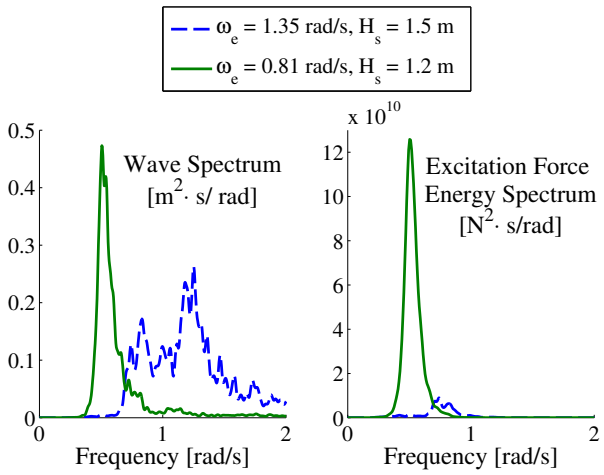

Fig. 4. Wave spectra, and resulting excitation force spectra, of real data collected at the Belmullet test site, off the West coast of Ireland.

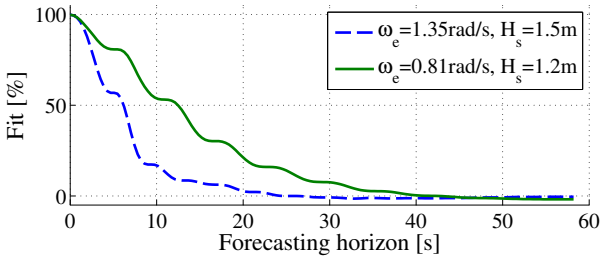

Fig. 5. AR predictor goodness of fit. The variance of the one-step ahead prediction error is $\sigma^2 = 1.75 \times 10^3$ for the higher frequency sea state (blue line) and $\sigma^2 = 1.86 \times 10^4$ for the low frequency swell (green line).

A linear AR model was identified and estimated to provide the real-time predictions of the excitation force, on the basis of the study presented in [9]. Fig. 5 shows the goodness of fit along the whole prediction horizon of 150 steps, for the two wave systems selected. As expected, the AR model is more accurate for the prediction of the sea state with a narrower bandwidth centered at a lower frequency (again, refer to [9]). More interestingly, however, note that the accuracy drops down very quickly and predictions seem reliable only for a fraction of the wave period (Fig. 5).

Based on the AR prediction model and on the non-causal law for the generation of the reference velocity, a spectral distribution of the variance of the error in the reference velocity is estimated, using Eq. (36). Fig. 6(a) and 6(d) compare such estimate with the real variance of the velocity error, $E\left\{\Delta v_{ref}^2[k]\right\}$. The latter is determined numerically from the difference between optimal velocity, calculated from ideal future values of the excitation force, and the velocity resulting from the use of predicted values. The estimated spectral model seems to describe quite accurately the distribution of the error's variance, particularly within the band of frequencies were the excitation force (and therefore the velocity) is significant. It is quite over-conservative, though, at frequencies where there is no excitation force, which comes

from the fact that a constant variance (white noise) is supposed to be the input of such stochastic model. The one-step ahead prediction error of the excitation force, in fact, is actually only a band-limited white noise, within the frequencies where the excitation force is contained, while it is practically zero elsewhere.

Note that the spectral model, $|G(e^{\jmath\omega})|^2$, is such that the prediction error is significantly attenuated in the range of frequencies between approximately 0.4 and $1\,rad/s$, while it is amplified at lower and higher frequencies. This band is strictly related to the systems radiation and to the frequency domain reference generation function, $H_{opt}(\omega)$, as it can be seen in Fig. 7. Moreover, the excitation force is usually contained mostly within this band of frequencies, as any higher-frequency components are filtered down by the excitation transfer function, Fig. 3(b), whose cut-off frequency is related to the bandwidth of the radiation resistance [1], $B(\omega)$, and therefore to $H_{opt}(\omega)$. In essence, any sea state components at high frequencies are significantly attenuated by the system's excitation properties, such that the error in the velocity reference, although amplified, would be not be very significant at those frequencies.

As regards the power, the losses due to the use of a wrong reference velocity can be determined through the spectral model proposed in section III-C. From Eq. (42), the average power loss, in the frequency domain, is proportional to the radiation resistance of the system multiplied by the spectral density of the error in the reference velocity. As can be seen in Figs. 6(b) and 6(e), given the resonant behavior of the radiation resistance, eventual errors at higher and lower frequencies than the radiation bandwidth are attenuated.

More insight can be gained from Figs. 6(c) and 6(f), which express the spectral density of the velocity error (real and estimated) with respect to the variance distribution of the optimal velocity. As from Eq. (43), this also expresses the ratio between power lost and optimal absorbed power. In absolute terms, the average power lost within the band of resonance of the system radiation is significant, but in relative terms such loss is very small. On the other end, the relative power loss at low and high frequencies is quite significant, but that's only because the ideal power absorption is almost zero at those frequencies, due to the aforementioned absence of excitation force components.

In order to have an idea of the cumulated effect of the excitation-force prediction error on the actual power produced, the spectral densities were integrated, over the frequencies were the model matches the actual data well. The total variance of the error in the velocity reference, over the variance of the optimal velocity is:

$$\begin{aligned} \frac{E\left\{\Delta v^2_{opt,1}[k]\right\}}{E\left\{v^2_{opt,1}[k]\right\}} &\approx 0.29 \\ \frac{E\left\{\Delta v^2_{opt,2}[k]\right\}}{E\left\{v^2_{opt,2}[k]\right\}} &\approx 0.13, \end{aligned} \tag{45}$$

wher the subscripts 1 and 2 refer, respectively to the low-frequency and higher-frequency sea states. Considering that the accuracy of the predictions is only acceptable over a short part of the future time horizon utilised for the velocity calculation (almost 60 seconds), note that the reference velocity error is quite small. As regards the average power:

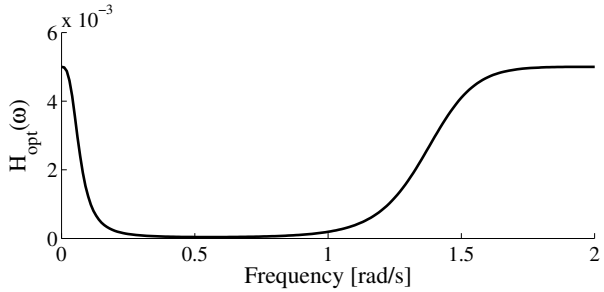

Fig. 7. Non-causal transfer function $H_{opt}(\omega) = 1/[2B(\omega) + 2K_f]$ utilised to generate the optimal reference velocity from the excitation force, as from Eq. (7).

$$\begin{aligned} \frac{E\left\{\Delta P_{opt,1}[k]\right\}}{E\left\{P_{opt,1}[k]\right\}} &\approx 0.085 \\ \frac{E\left\{\Delta P_{opt,2}[k]\right\}}{E\left\{P_{opt,2}[k]\right\}} &\approx 0.40. \end{aligned} \tag{46}$$

For the sea state 1, that is the low frequency swell, only a 8.5% drop in absorbed power is experienced due to the error in the excitation force. On the other hand a 40% power is lost due to the prediction error in the case of the sea state centered at higher frequencies. Such results are surprising, considering that the relative error in the velocity reference, Eq. (45), is bigger (more than double) for the low frequency swell. However, from comparison of Fig. 4 and Fig. 6(c), it can be noticed that most of the power for the sea state 2 is actually concentrated at frequencies where the power loss, in relative terms, gets bigger.

V. Conclusion

This paper proposed a model for the estimation of the effects that the wave-excitation-force prediction error has on the reference velocity that is calculated from a non-causal control of a WEC, aimed at maximum power absorption. In particular, the spectral density of the error in the reference velocity, and the average power loss, are expressed as stochastic models driven by a white noise, representing the one-step ahead prediction error of the excitation force. The model can be directly derived from the parameters of the predictor and from the non-causal reference generator, with no additional information about the excitation force required. Simulation results have shown how such model is able to give an accurate estimation of the frequency distribution of the variance of the velocity errors and of the average absorbed power, at least within the band of frequencies where the excitation force is contained.

The value of the proposed frequency domain model is critical for the design of a real-time controller, based on a non-causal calculation, whose performance is as robust as possible

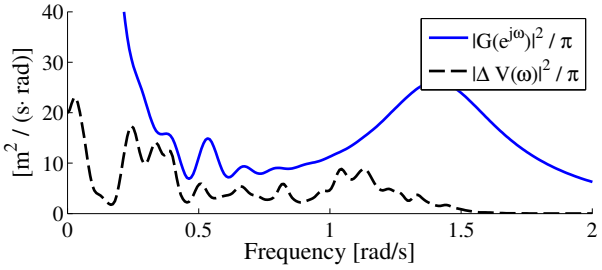

(a) Power spectral density of reference velocity error.

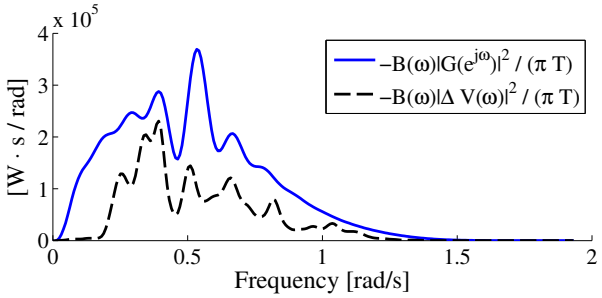

(b) Distribution in the frequency of average lost power due to reference velocity error.

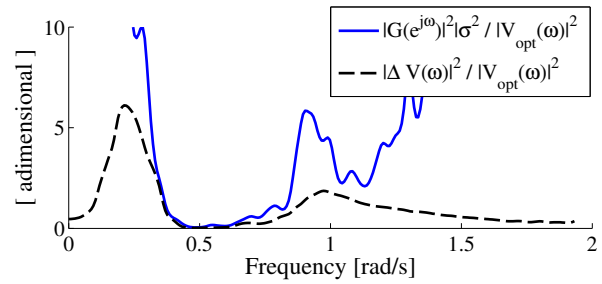

(c) Relative error of velocity reference with respect to optimal reference. Ratio equals the relative power lost.

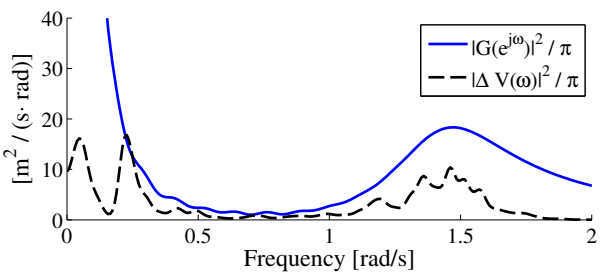

(d) Power spectral density of reference velocity error.

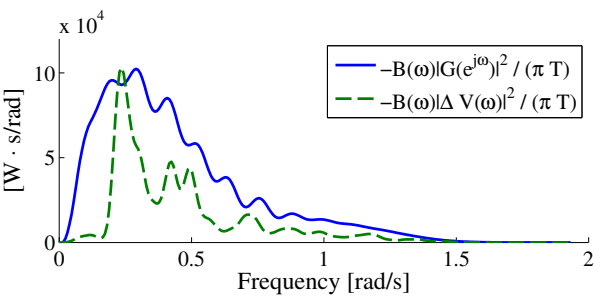

(e) Distribution in the frequency of average lost power due to reference velocity error.

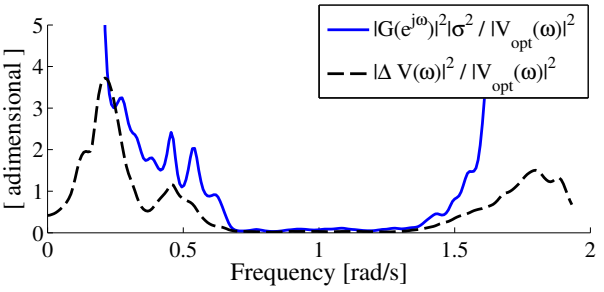

(f) Relative error of velocity reference with respect to optimal reference. Ratio equals the relative power lost.

Fig. 6. Spectral density estimates (blue solid line) against real spectral densities (dashed black line) of errors in the reference velocity and absorbed power, due to errors in the prediction of the excitation force: *(a), (b), (c)* refer to the sea state at concentrated at low frequencies; *(d), (e), (f)* refer to the wider sea state at higher frequencies.

to inevitable prediction errors. It was shown, in fact, how prediction errors at different frequencies can have different impact on the error in the reference velocity. In the same way, errors in the reference velocity, at certain frequencies, are significantly attenuated by the control and system dynamics, so that they do not affect the power absorption. Important specifications can therefore be derived for the wave-excitation-force prediction model, so that a maximum desired error is achieved within a certain band of frequencies, but also for the lower level loop. In particular, the closed loop transfer function can be shaped such that velocity errors at certain band of frequencies are attenuated.

While the numerical example utilised in the paper was based on reactive control, it was shown how the proposed model can be adapted for different non-causal control strategies, such as MPC, although further work needs to be done in this direction.

ACKNOWLEDGMENT

The authors are grateful to the Irish Marine Institute for providing real sea observations. This work is supported by the Irish Research Council for Science, Engineering and Technologies (IRCSET) under the Embark Initiative.

REFERENCES

[1] J. Falnes, *Ocean Waves and Oscillating Systems*. Cambridge University Press, 2002.

[2] G. Bacelli, J.-C. Gilloteaux, and J. Ringwood, "A predictive controller for a heaving buoy producing potable water," *Proc. of the European Control Conference (ECC) 2009, Budapest, Hungary*, pp. 3755–3760, 2009.

[3] J. Cretel, A. W. Lewis, G. Lightbody, and G. P. Thomas, "An application of model predictive control to a wave energy point absorber," *Proc. Of the IFAC Conference on Control Methodologies and Technology for Energy Efficiency (CMTEE) 2010, Portugal*, 2010.

[4] J. Hals, J. Falnes, and T. Moan, "Constrained optimal control of a heaving buoy wave-energy converter," *Journal of Offshore Mechanics and Arctic Engineering*, vol. 133, 2011.

[5] M. Belmont, J. Horwood, R. Thurley, and J. Baker, "Filters for linear sea-wave prediction," *Ocean Engineering*, vol. 33, pp. 2332–2351, 2006.

[6] J. Tedd and P. Frigaard, "Short term wave forecasting, using digital filters, for improved control of wave energy converters," *Proc. of Int. Offshore and Polar Eng. (ISOPE) Conf.*, pp. 388, 394, 2007.

[7] H. Van Den Boom, "Owme project makes technological breakthrough," *Marin Report*, 2009.

[8] F. Fusco and J. Ringwood, "A study on short-term sea profile prediction for wave energy applications," *Proceedings of the 8th European Wave and Tidal Energy Conference (EWTEC)*, pp. 756–765, Uppsala, Sweden, 2009.

[9] ——, "Short-Term Wave Forecasting for Real-Time Control of Wave Energy Converters," *IEEE Trans. on Sustainable Energy*, vol. 1, no. 2, pp. 99–106, 2010.

[10] ——, "Quantification of the prediction requirements in reactive control of wave energy converters," *Proc. of 18th World Congress of the International Federation of Automatic Control (IFAC), Milano, Italy*, 2011.

[11] J. Falnes, "Optimum control of oscillation of wave-energy converters," *Paper no. 2 in Annex Report B1 to the JOULE project "Wave Energy Converters: Generic Technical Evaluation Study"*, 1993.

[12] U. A. Korde, "Efficient primary energy conversion in irregular waves," *Ocean Eng.*, vol. 26, pp. 625–651, 1999.

[13] A. Babarit, D. G., and A. Clement, "Comparison of latching control strategies for a heaving wave energy device in random sea," *Applied Ocean Research*, vol. 26, pp. 227–238, 2004.

[14] J. Hals, J. Falnes, and T. Moan, "A comparison of selected strategies for adaptive control of wave energy converters," *Journal of Offshore Mechanics and Arctic Engineering*, vol. 133, no 3, 2011.

[15] F. Fusco and J. Ringwood, "Suboptimal causal reactive control of wave energy converters using a second order system model," *Proceedings of the International Society of Offshore and Polar Engineers (ISOPE), Maui, USA*, 2011.

[16] U. A. Korde, "On control approaches for efficient primary energy conversion in irregular waves," *Proceedings of IEEE Oceanic Engineering Society OCEANS'98*, vol. 3, pp. 1427–31, 1998.

[17] F. Fusco, J.-C. Gilloteaux, and J. Ringwood, "A Study on Prediction Requirements in time-domain Control of Wave Energy Converters," *Proc. of Control Applications in Marine Systems (CAMS), Germany*, 2010.

[18] T. Perez and T. I. Fossen, "A matlab toolbox for parametric identification of radiation-force models of ships and offshore structures," *Modeling, Identification and Control*, vol. 30, pp. 1 – 15, 2009.

[19] ——, "Practical aspects of frequency-domain identification of dynamic models of marine structures from hydrodynamic data," *Ocean Engineering*, vol. 38, pp. 426–435, 2011.

[20] K. J. Astrom, *Introduction to Stochastic Control Theory*. Dover Publications, Inc., 2006.

[21] WAMIT Inc., "Wamit," *MA, USA, version 6.4*, 2008.